Experimental Animals
Exp. Anim. 70(3), 333–343, 2021

Original

Generation of avian-derived anti-B7-H4 antibodies exerts a blockade effect on the immunosuppressive response

Tsai-Yu LIN[1)]*, Tsung-Hsun TSAI[2)]*, Chih-Tien CHEN[3,4)], Tz-Wen YANG[1)], Fu-Ling CHANG[5)], Yan-Ni LO[1)], Ting-Sheng CHUNG[2)], Ming-Hui CHENG[6)], Wang-Chuan CHEN[7,8)], Keng-Chang TSAI[10,11)] and Yu-Ching LEE[1,9,11–13)]

[1)]*TMU Research Center of Cancer Translational Medicine, Taipei Medical University, No. 250, Wuxing Street, Taipei 11031, Taiwan*
[2)]*Department of Psychiatry, Kaohsiung Armed Forces General Hospital, No.2, Zhongzheng 1st Rd., Lingya Dist., Kaohsiung 80284, Taiwan*
[3)]*Institute of Medicine, Chung Shan Medical University, No.110, Sec.1, Jianguo N. Rd., Taichung 40201, Taiwan*
[4)]*Department of Surgery, Taichung Veterans General Hospital, No.1650, Taiwan Boulevard Sect. 4, Taichung 40705, Taiwan*
[5)]*Ph.D. Program for Cancer Molecular Biology and Drug Discovery, College of Medical Science and Technology, Taipei Medical University and Academia Sinica, No. 250, Wuxing Street, Taipei 11031, Taiwan*
[6)]*Department of Laboratory Medicine, Lo-Hsu Medical Foundation, Lotung Poh-Ai Hospital, No. 83, Nanchang St., Luodong Township, Yilan 26546, Taiwan*
[7)]*The School of Chinese Medicine for Post Baccalaureate, I-Shou University, No.1, Sec. 1, Syuecheng Rd., Dashu District, Kaohsiung 84001, Taiwan*
[8)]*Department of Chinese Medicine, E-Da Hospital, No.8, Yida Rd., Jiaosu Village Yanchao District, Kaohsiung 82445, Taiwan*
[9)]*Ph.D. Program for Cancer Molecular Biology and Drug Discovery, College of Medical Science and Technology, Taipei Medical University, No. 250, Wuxing Street, Taipei 11031, Taiwan*
[10)]*National Research Institute of Chinese Medicine, Ministry of Health and Welfare, No. 155-1, Sec. 2, Linong St., Beitou District, Taipei 11221, Taiwan*
[11)]*Ph.D. Program in Medical Biotechnology, College of Medical Science and Technology, Taipei Medical University, No. 250, Wuxing Street, Taipei 11031, Taiwan*
[12)]*Ph.D. Program in Biotechnology Research and Development, College of Pharmacy, Taipei Medical University, No. 250, Wuxing Street, Taipei 11031, Taiwan*
[13)]*Biomedical Commercialization Center, Taipei Medical University, No. 250, Wuxing Street, Taipei 11031, Taiwan*

Abstract: For highly conserved mammalian protein, chicken is a suitable immune host to generate antibodies. Monoclonal antibodies have been successfully targeted with immunity checkpoint proteins as a means of cancer treatment; this treatment enhances tumor-specific immunity responses through immunoregulation. Studies have identified the importance of B7-H4 in immunoregulation and its use as a potential target for cancer treatment. High levels of B7-H4 expression are found in tumor tissues and are associated with adverse clinical and pathological characteristics. Using the phage display technique, this study isolated specific single-chain antibody fragments (scFvs) against B7-H4 from chickens. Our experiment proved that B7-H4 clearly induced the inhibition of T-cell activation. Therefore, use of anti-B7-H4 scFvs can effectively block the exhaustion of immunity cells and also stimulate and activate T-cells in peripheral blood mononuclear cells. Sequence analysis revealed that two isolated scFv S2 and S4 have the same VH complementarity-determining regions (CDRs) sequence. Molecule docking was employed to simulate the complex structures of scFv with B7-H4 to analyze the interaction. Our findings revealed that both scFvs employed CDR-H1 and CDR-H3 as main driving forces and had strong binding effects with the B7-H4. The affinity of scFv S2 was better because the CDR-L2 loop of the scFv S2 had three more hydrogen

(Received 25 November 2020 / Accepted 7 February 2021 / Published online in J-STAGE 15 March 2021)
Corresponding authors: K.-C. Tsai. e-mail: tkc@nricm.edu.tw
Y.-C. Lee. e-mail: ycl@tmu.edu.tw
**These authors contributed equally in this work.*
Supplementary Figure: refer to J-STAGE: https://www.jstage.jst.go.jp/browse/expanim

bond interactions with B7-H4. The results of this experiment suggest the usefulness of B7-H4 as a target for immunity checkpoints; the isolated B7-H4-specific chicken antibodies have the potential for use in future cancer immunotherapy applications.
Key words: B7-H4, immunity checkpoint protein, molecule docking, phage display technique, single-chain antibody fragment

Introduction

Immunotherapy has changed conventional cancer therapy strategies. Therapeutic antibodies that inhibit programmed death ligand 1 (PD-L1)/ programmed cell death protein 1 (PD-1) interactions can reactivate anti-tumor immunity responses [1]. In cancer therapy, less than 30% of patients demonstrate responses to treatments that inhibit PD-L1/PD-1 interactions. PD-L1 expression on cancer cells is an effective and commonly used assessment indicator for immunotherapy. However, most patients have low PD-L1 protein expression on cancer cells, which results in poor immunotherapy responses [2]. Therefore, research on the development of other potential immune checkpoint protein inhibitors is necessary. The V-set domain containing T-cell activation inhibitor 1 (VTCN1) is generally referred to as B7-H4, B7-S1, or B7x; it is a key B7 family member [3]. B7-H4 proteins in humans and mice are 90% similar, indicating B7-H4 is a highly conserved protein [4]. The protein has been found capable of affecting cytokine secretion, T-cell activation, and cytotoxicity abilities [5, 6]. B7-H4 has been found in human tumors; in addition to serving as a potential treatment indicator [7–10], soluble B7-H4 has been recognized as a possible biomarker for cancer diagnosis [11, 12]. Clinical research also revealed that relative to B7-H4+ tumors, B7-H4− tumors are larger (on average) and occur in patients with higher TNM stages [13]. In general, B7-H4 expression is low in immune cells. The *in vitro* expression of B7-H4 can be induced through stimulation (e.g., LPS, IFN-γ), implying that B7-H4 might play a key role in the tumor microenvironment. Research has revealed that the tumor-associated macrophages in clinical patients with ovarian carcinoma exhibited high B7-H4 protein level and an increase in Treg cells. These patients had low survival rates [14]. In renal cell carcinoma, B7-H4 mRNA and protein expression were increased due to stimulation by inflammatory mediators [15]. This indicates that in tumor microenvironments, the cytokine network may regulate B7-H4 expression in cancer cells and in infiltrating immune cells. Similar findings have been published in research on lung cancer in humans. TAMs secrete IL-10, TNF-α, and IFN-γ to induce B7-H4 expression in lung cancer cells, thereby generating an immune escape response [5]. Accordingly, studies have supported the importance of B7-H4 in cancer development and in immunotherapy.

Hybridoma is a conventional monoclonal antibody production protocol. Despite being a widely known and mature experimental method, the protocol has a complicated production process, is time-consuming, and presents many challenges [16]. The first recombinant antibody library was established in 1989, which involved the use of phage display to create an effective, convenient, and rapid path to produce monoclonal antibodies. This effective *in vitro* screening method allows for the enrichment of specific antibodies from complicated phage antibody libraries [17]. Clinical applications and research have employed this technique to develop various antibodies as target therapy medicines [18, 19]. To facilitate such development, small mammals such as mice and rabbits are commonly used as immune animals to induce humoral antibody response. However, mammal proteins, which have highly conserved sequences, often cannot induce highly potent immune responses due to tolerance developed in the immunity process. This problem has limited and obstructed the progress of research. Because of the species difference, chickens can induce stronger-than-usual humoral responses. Thus, the use of chickens as immune hosts can overcome typical experimental challenges. Unlike mammals, which have two light chains isotypes (kappa and lambda), chickens only have the lambda light chain, which is conducive to the construction of antibody libraries and effective screening [20]. Additionally, single-chain variable fragments (scFvs) with the immunoglobulin scaffold of chickens generally have high expression levels in the bacterial expression system [21]. Studies have proven that chicken scFv antibodies have various potential applications [22, 23]. In the future, chicken scFv antibodies must be humanized for clinical applications, which is an obstacle that can be overcome with antibody construction technology [24].

In the present study, high-specificity chicken scFv antibodies were manufactured with binding specificity to B7-H4 protein, which has highly conserved sequences in mammals. The blockade effect of the antibody was

validated; these antibodies successfully bonded with B7-H4 protein to protect the activation responses of immunity cells. Additionally, we used molecule docking to predict the docking position of the antibodies with the B7-H4 protein, and in this paper, we discuss the potential antigenic determinants on B7-H4 proteins and the potential interactions between antibody complementarity-determining region (CDR) loops and B7-H4 protein. The results of this research can contribute to the development of antibody medicines for immune checkpoint protein B7-H4 and can be further applied to future clinical applications.

Materials and Methods

Chicken immunization and library construction

Female white leghorn chickens were immunized through intramuscular injection of 50 μg of recombinant B7-H4 protein (Phe29 to Ala258) (Sino Biological Inc., Beijing, China) mixed with an adjuvant (Sigma-Aldrich, Inc., St. Louis, MO, USA). Three additional immunizations were performed at intervals of 7 days. During the immunization, we used Freund's Complete Adjuvant (FCA) for the first time and Freund's Incomplete Adjuvant (FIA) for the other times. The spleens of the chickens were harvested 7 days after the final immunization to construct an scFv antibody library. The library construction method followed published protocols with minor modifications (20). The chickens were maintained with care, and all animal experiments complied with ethical standards; protocols were reviewed and approved by the Animal Use and Management Committee of Taipei Medical University (IACUC number: LAC-2018-0391).

Biopanning

The clone in the constructed scFv antibody library with binding specificity to B7-H4 protein can be enriched and isolated through panning. The recombinant B7-H4 protein was coated in the well of a microtiter plate at 4°C overnight. The next day, the B7-H4 protein was removed, and the well was blocked with 3% bovine serum albumin (BSA) at room temperature for 1 h. Then, recombinant phage particles (10^{11}) from the library were added to the well and incubated at room temperature for 2 h. Unbound phages were subsequently removed, and the well was washed through pipetting with PBST (phosphate buffered saline with 0.05% Tween 20) 10 times. Bound phages were eluted with 0.1 M HCl-glycine (pH 2.2)/0.1% BSA elution buffer and neutralized with 2 M Tris base buffer. The eluted phages were used to infect *Escherichia coli* strain ER2738 immediately for recombinant phage amplification. Amplified phages were precipitated and recovered according to the described method and used in the next round of panning [17]. The panning procedure was repeated four times. After panning, all library DNA was purified and transformed into *E. coli* strain TOP 10F' (Invitrogen, a nonsuppressor strain) for scFv expression. The expressed scFv were further purified with Ni^{2+}-charged sepharose according to the manufacturer's instructions (GE Biosciences, Pittsburgh, PA, USA).

Sequence analysis

To sequence the scFv clones of interest, a primer ompseq (5'-AAGACAGCTATCGCGATTGCAGTG-3') complementary to the outer membrane protein A (ompA) signal sequence in front of the light chain variable region was used. International ImMunoGeneTics information system/V-QUEry and Standardization (http://imgt.org) were used to compile and analyze the sequence data in accordance with the germline genes.

Enzyme-linked immunosorbent assay

The wells of the microtiter plate were coated with recombinant B7-H4 protein (0.5 μg/well) at 4°C overnight. After blocking with 5% skim milk, the scFv or phage was added to the wells and incubated for 1 h at room temperature. The wells were washed with PBST, and the bound scFv or phage was then detected and developed using horseradish peroxidase (HRP)-conjugated goat antichicken light-chain antibodies (Bethyl Laboratories, Inc., Montgomery, TX, USA) or HRP-conjugated anti-M13 antibodies (GE Healthcare Life Science, Pittsburgh, PA, USA). Finally, 3,5,5-tetramethubezidine dihydrochloride substrate (TMB) was added for signal development. The reaction was stopped by adding 1 N HCl, and absorbance was measured at 450 nm.

For peptide enzyme-linked immunoabsorbent assay (ELISA), the biotin-conjugated peptides BS1pep-p8 (KNVQLTDA) and BS2pep-p17 (VIQWLKEGVLGLVHEFK), representing the two linear epitopes of B7-H4, were synthesized (Kelowna International Scientific Inc., New Taipei City, Taiwan). Anti-B7-H4 scFv S2 and S4 antibodies were individually coated on a 96-well microplate at 4°C overnight. After blocking with 3% BSA, BS1pep-p8 and BS2pep-p17 were added to scFv S2 and scFv S4 for incubation, respectively. Next, peroxidase-conjugated streptavidin (Jackson ImmunoResearch Laboratories, Inc., West Grove, PA, USA) was used to bind biotin-conjugated peptides for detection. Finally, a TMB substrate was added for development, and the reaction was stopped by adding 1 N HCl. The absorbance was measured at 450 nm.

Western blotting

The recombinant B7-H4 protein was transferred onto nitrocellulose membranes (GE Healthcare Life Sciences) after sodium dodecyl sulfate-polyacrylamide gel electrophoresis (SDS-PAGE) to determine binding reactivity, which was measured using purified scFv antibodies. The membranes were blocked with 5% skim milk and then incubated with scFv at room temperature for 1 h. After a PBST wash process, the membranes were detected and developed with HRP-conjugated goat anti-chicken light-chain antibodies. Finally, diaminobenzidine substrate was added for color development until the desired color intensity was reached.

T cell activating assay

In the assay, a commercial anti-CD3 antibody (eBioscience, Inc., Houston, TX, USA) was used to conduct T-cell activation and proliferation. The peripheral blood mononuclear cells (PBMCs) of healthy persons used in the experiment were purchased from a commercial supplier (STEMCELL Technologies Inc., Cambridge, MA, USA). Before the experiment, anti-CD3 monoclonal antibodies were coated on 96-well tissue culture plates at 4°C overnight. The next day, PBMCs were labeled with 0.5 μM CFSE (eBioscience, Inc.) and incubated with a testing scFv at room temperature for 30 min. Then, the anti-CD3 antibodies were removed, and the treated PBMCs were distributed in the antibody-coated wells for incubation. T-cell responses were analyzed 5 days after activation through flow cytometry. This analysis was based on the cell-labeling CSFE signals to reflect T-cell activation responses.

Molecular docking

To investigate how chicken scFvs interact with B7-H4, scFv 2S and 4S structural models were developed in accordance with the protocols of the Antibody Modeling Cascade modules in Discovery Studio v. 2020 (BIOVIA Inc., San Diego, CA, USA). The light chain of the scFv S2 and S4 models were generated using the crystallographic structure of the anti-ptau (PDB ID: 4GLR) and the anti-Bla g1 (PDB ID: 4OUO) as scFv structural templates, respectively. Moreover, the same heavy chain of the scFv models was used to construct the x-ray structure of antiprostate specific antigen antibodies (PDB ID: 4P49). In addition, the framework of the scFv S2 and S4 models was built using the x-ray structures of the PDB IDs of 4GLR and 4P49, respectively. We developed our complex structural model of the scFv–B7-H4 interaction on the antibody–antigen docking program ZDOCK [25] by using default parameters and evaluating shape complementarity and desolvation energy to obtain an scFv–B7-H4 complex. We selected the PDB ID of 4GOS to be the antigen of the three-dimensional x-ray crystallographic structure of B7-H4. To obtain a reliable complex structure, we used an RDOCK program to refine the docked protein poses of cluster 1 from ZDOCK by performing energy minimization in CHARMm. Finally, the rational antibody–antigen complex model satisfied the CDRs of the scFv S2 and S4 antibodies interacting with the B7-H4 binding site at the antigen-antibody interface.

Results

Chicken immunization with recombinant B7H4 protein

Comparison of protein sequences revealed that the B7-H4 proteins in humans (AAH74729.1) and mice (AAH32925.1) are 90% similar. For highly conserved proteins, such as B7-H4, we selected chickens for specific humoral immune responses. Figure 1 indicates that the poly-IgY antibody purified from egg yolks of an immunized chicken, after serial dilution, has high-potency binding with recombinant B7-H4 protein (Fig. 1A). For the control group, recombinant B7-H4 protein was used for mouse immunization, and an immunity response was not induced (Fig. 1B). Figure 1 details the limitations of highly conserved proteins in animal immunity and highlights the advantage of using chickens as immune hosts due to the species difference; this allows for the successful generation of high-potency antibody responses in chickens.

ScFv antibody library construction and biopanning

To produce an anti-B7-H4 monoclonal antibody with neutralizing capabilities, we used the recombinant B7-H4 protein for chicken immunization. After high-potency antibody responses had been induced, the chicken was sacrificed, and a highly complicated phage display scFv antibody library (2×10^8) was established and subjected to panning against the B7-H4 protein. Figure 2A indicates that relative to the wild-type M13 phage, the eluted phage titer significantly increased with the number of panning rounds during the experiment conducted with library phage. After the fourth round of panning, the eluted phage titer had a 290-fold increase, indicating that anti-B7-H4-specific phage had been enriched in the library. The phage library was amplified after each round of panning and subjected to the phage ELISA test against the B7-H4 protein. Relative to the initial phage library, which did not exhibit binding responses, the results revealed that after the second round of panning, the library phage generated significant binding signals (Fig. 2B).

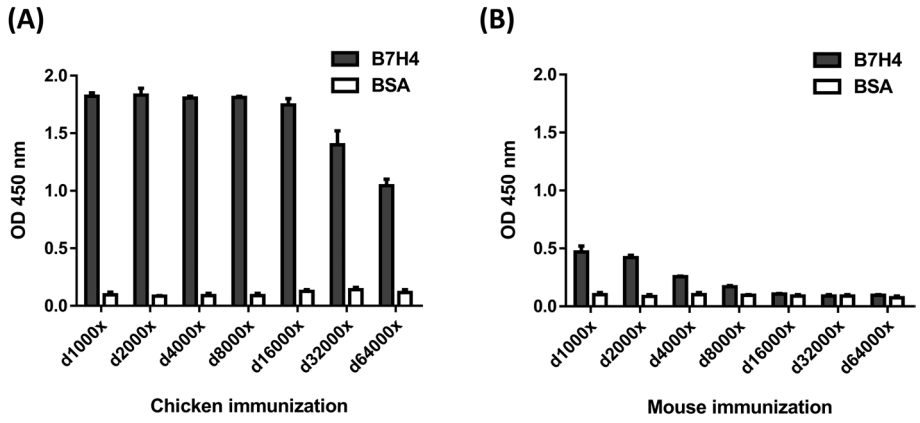

Fig. 1. Humoral antibody response in chicken after immunization of recombinant B7-H4 protein. (A) Chicken immunization using recombinant B7-H4 protein and testing the binding effect of poly-IgY antibody purified from egg yolks of an immunized chicken with the recombinant B7-H4 protein under each serial dilution concentration. (B) Mouse immunization using recombinant B7-H4 protein to test the binding effect of the B7-H4-specific antibody in the mouse serum under each serial dilution concentration.

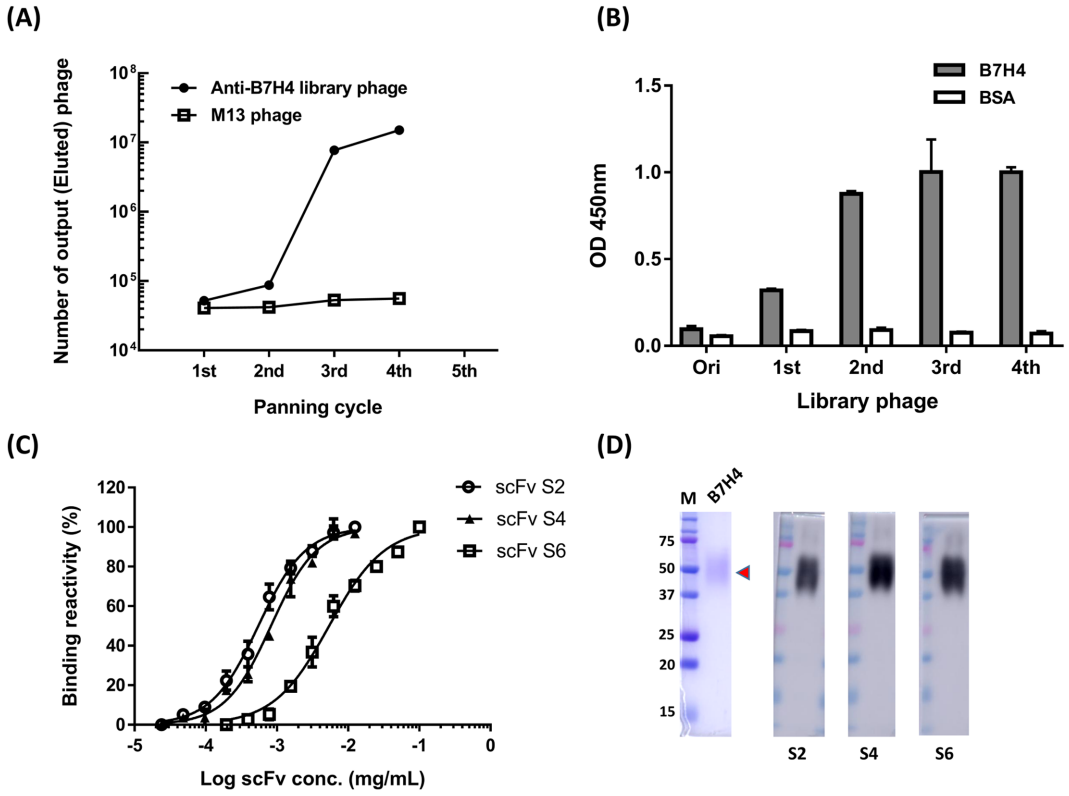

Fig. 2. Biopanning and single colony analysis. (A) Eluted phage number of the anti-B7-H4 library phage calculated after each panning round, which represents the number of specific phages binding to B7-H4 protein in each panning round. M13 represents wild-type phages and is the negative control. (B) Phage ELISA testing on the amplified phage library after each panning round to test binding to B7-H4 protein. (C) Serial dilution on the three representative scFvs to test the binding reactivity to B7-H4 protein. (D) Western blotting test of the binding effect of the three representative scFvs on recombinant B7-H4 protein. The red arrow indicates that the molecular weight of recombinant B7-H4 protein is approximately 50 kDa.

Single colony analysis

After panning, 15 clones were randomly selected for single-colony analysis. The sequencing results revealed that similar sequences were repeated, which was the result of the enriched expression of the specific phage in the panning process. The 15 clones exhibited three sequences, which are represented as clones S2, S4, and S6; Fig. 2C depicts the situation following expression of the representative scFvs, specifically when serial dilution was performed on the clones to test the B7-H4 bind-

ing effect of each concentration of scFv. Results revealed that clone S6 had a poor binding effect; clones S2 and S4 had higher binding effects, accounting for EC_{50} of approximately 22 and 33 nM, respectively. After the recombinant B7-H4 protein had been subjected to electric transfer, a Western blotting test was performed on the protein to test the binding reactivity of scFvs. The results revealed that all three represented scFvs were capable of identifying denatured B7-H4 proteins (Fig. 2D); this indicates that the three scFvs identified B7-H4 by recognizing the liner epitope structure in B7-H4.

ScFv S2 and S4 can block the effect of B7H4-induced T-cell exhaustion in PBMC

To confirm whether the extracted anti-B7-H4 scFv fragment exhibited the blockade effect on the immunosuppression response induced by B7-H4 protein, we selected scFvs S2 and scFv S4, both of which exhibit high binding capabilities, for antibody testing. During testing, human PBMCs were activated with anti-CD3 antibodies, and B7-H4 proteins and antibodies were added to determine their effects and observe the T-cell response. Figure 3A displays the groups to which were added anti-CD3 antibodies that exhibited significant T-cell activation and cluster responses; after B7-H4 protein had been added, the clustering response was inhibited. Additionally, the activation and clustering of regenerative T-cells were observed in the results of groups to which scFv S2 and scFv S4 had been separately added. This implies that scFv S2 or scFv S4 bound to B7-H4 protein can effectively neutralize the immunosuppression response induced by B7-H4 proteins, thus enabling T-cells to retain their activation status. Similar responses were observed in another cell experiment, as presented in Fig. 3B. CSFE-stained PBMCs to which were added anti-CD3 antibodies effectively induced the activation of T-cells, which further prompted cell proliferation. This response was inhibited when B7-H4 proteins were added. In the experiment, separately adding scFv S2 and scFv S4 effectively blocked the effect of the B7-H4 protein, thereby preventing the activation of T-cells from being inhibited. After calculation and normalization, we determined that the effects of scFv S2 and scFv S4 enabled the retention of 56% and 51% of the original T-cell activity after activation, respectively (Fig. 3C).

Epitope prediction and analysis of B7H4

To predict possible epitopes on the B7-H4 protein surface, we compared the protein structure of the B7-H4 protein (PDB ID: 4GOS) with the B7-H1 (PD-L1) protein (PDB ID: 4ZQK), which is in the same protein family. By superimposing the protein structures, as presented in Fig. 4A, it was observed that despite only having 50.8% similarity, the two proteins had highly similar basic structures because they were from the same family. Due to the lack of clear data on the B7-H4 complex structure, we employed the Binding Site Prediction software of Discovery Studio to predict possible positions where protein binding may occur on B7-H4 proteins. Analysis revealed that the amino acid on the surface of B7-H4 protein tends to generate two aggregation sites (in red boxes), which are represented as BS1 and BS2. These two predicted aggregation sites are highly likely to generate protein–protein interactions. However,

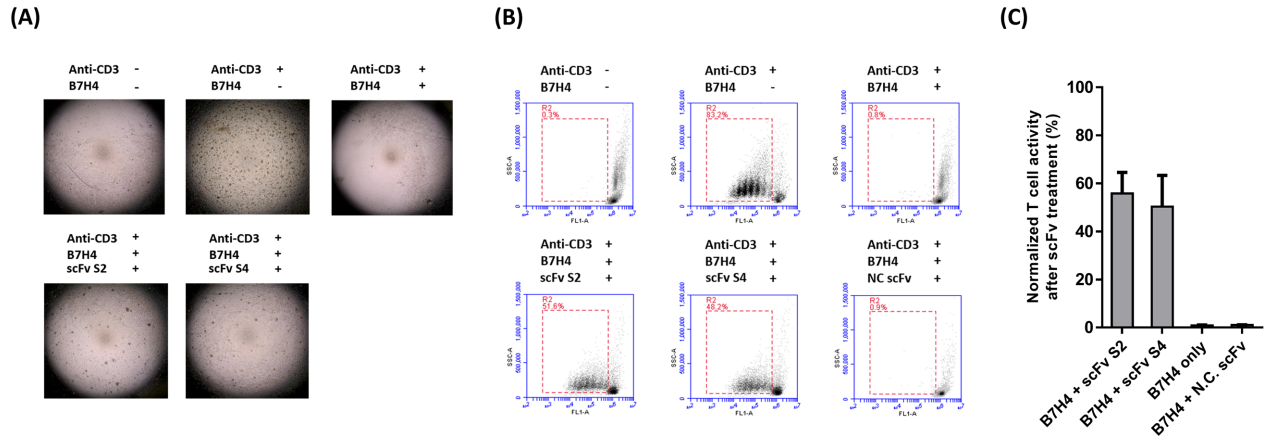

Fig. 3. Anti-B7-H4 scFv has a blockade effect on T-cell exhaustion caused by B7-H4 protein. (A) Inclusion of B7-H4 protein and the assigned scFv in the cultivation of PBMCs of healthy persons for 5 days, as observed under a microscope. Anti-CD3 antibody was used to stimulate the activation of T-cells, and activated T-cells then proliferated and clustered. (B) Inclusion of B7-H4 protein and the assigned scFv in the cultivation of CSFE-stained PBMCs for 5 days, followed by flow cytometry assay for analysis. Activated T-cells proliferated and caused fluorescent signal changes. An unrelated scFv (NC), under the same cultivation conditions, was included as the negative control for the antibody response. (C) Quantified activation response results for T-cells in the CSFE-stained PBMCs after scFv processing using normalized percentages.

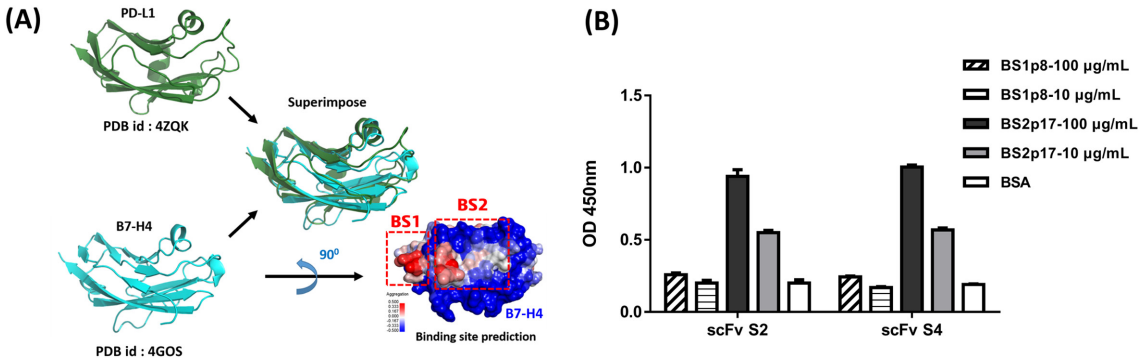

Fig. 4. Structural comparison between B7-H4 and PD-L1 proteins and antibody binding position confirmation. (A) Superimposed analysis of the similarities between the protein structures of B7-H4 (PDB ID: 4GOS) and PD-L1 (PDB ID: 4ZQK). The Binding Site Prediction software of Discovery Studio was used to predict the possibility of protein–protein binding on the protein surface. Regions with higher aggregation value (red) are more likely to exhibit protein binding; regions with lower aggregation value (blue) are less likely to exhibit protein binding. The results predicted BS1 and BS2 to be the most likely epitope regions on B7-H4 protein. (B) ELISA testing to confirm the binding response of the designed peptides BS1p8 and BS2p17, which were designed in accordance with the predicted epitope regions on B7-H4 protein (BS1 and BS2), with both scFv S2 and scFv S4.

to further validate whether scFv S2 and scFv S4 bind to the predicted key sites, we designed two peptides according to the corresponding amino acid sequence of the two sites, respectively BS1pep-p8 and BS2pep-p17, to simulate the reaction loop on B7-H4 molecules and test their binding with both scFv S2 and scFv S4. The experiment results revealed that scFv S2 and scFv S4 both bound to BS2pep-p17 but did not bind to BS1pep-p8 (Fig. 4B). Therefore, after using molecule modeling to construct the protein structure of scFv S2 and scFv S4, we used molecule docking to predict the binding model between scFv S2 and scFv S4 with B7-H4. From the predicted binding model, it was observed that despite the binding sites being near each other, the binding direction of scFv S2 and scFv S4 to B7-H4 was different due to differing scFv sequences. In both scFvs, B7-H4 proteins mainly interacted with the heavy chain variable domains. Through this binding effect, antibodies effectively blocked the interaction between B7-H4 and the corresponding proteins.

Molecule docking of scFvs with B7H4 molecule

Amino acid sequence analysis revealed that scFv S2 and scFv S4 have nearly identical VH sequences (121/122, 99.2% similarity), with the only difference being the amino acid positioned at FR1 (G18A). In the VL region, the key difference was evident in the CDR position, particularity at CDR3 (Fig. 5A). To construct the binding model for scFv S2 and scFv S4, we selected two published antibody sequences in chicken with the highest similarity from the Protein Data Bank as the structure model. The model of scFv S2 was obtained from the structures of PDB IDs 4GLR and 4P49, and the model of scFv S4 was obtained from the structures of PDB IDs 4P49 and 4OUO. By using homology modeling analysis, we simulated the structural model of scFv S2 as well as that of scFv S4. Based on the Peptide ELISA results, we determined that scFv S2 and scFv S4 recognized the possible epitopes on B7-H4 (Fig. 4), and by using molecule docking prediction analysis, we separately established the complex structures of scFv with B7-H4, and superimposed the structures (Fig. 5B). We discovered that the epitopes for scFv S2 and scFv S4 on B7-H4 are similar and that both scFvs have largely identical VH sequences. However, their difference in VL sequence resulted in the two scFvs binding to B7-H4 in different directions.

Interaction analysis between scFv S2 and B7H4 molecule

Antibody-antigen docking revealed that the CDRs of scFv S2, namely CDR-L1, CDR-L2, CDR-L3, CDR-H1, CDR-H2, and CDR-H3, were involved in the interaction of the epitope on B7-H4 with scFv S2 (Fig. 6). The Gly28 main chain on the CDR-L1 loop was involved in the Glu92 side chain of the B7-H4 epitope by a hydrogen bond. The side chains of Asn56, Asn57, and Asn65 of the CDR-L2 loop interacted with the B7-H4 epitope on three residues, namely Glu92, Ser91, and Glu89, through respective hydrogen bond. In addition, the CDR-L3 loop had a hydrophobic interaction between the side chains of Leu77 and Trp107. The main chain of Gly27 and the side chains of Thr29, Ser35, Ser36, and Tyr37 on the CDR-H1 loop interacted with those of Asn140, Asn142, and Lys129 through four hydrogen bonds and a hydrophobic interaction. The CDR-H2 loop did not interact

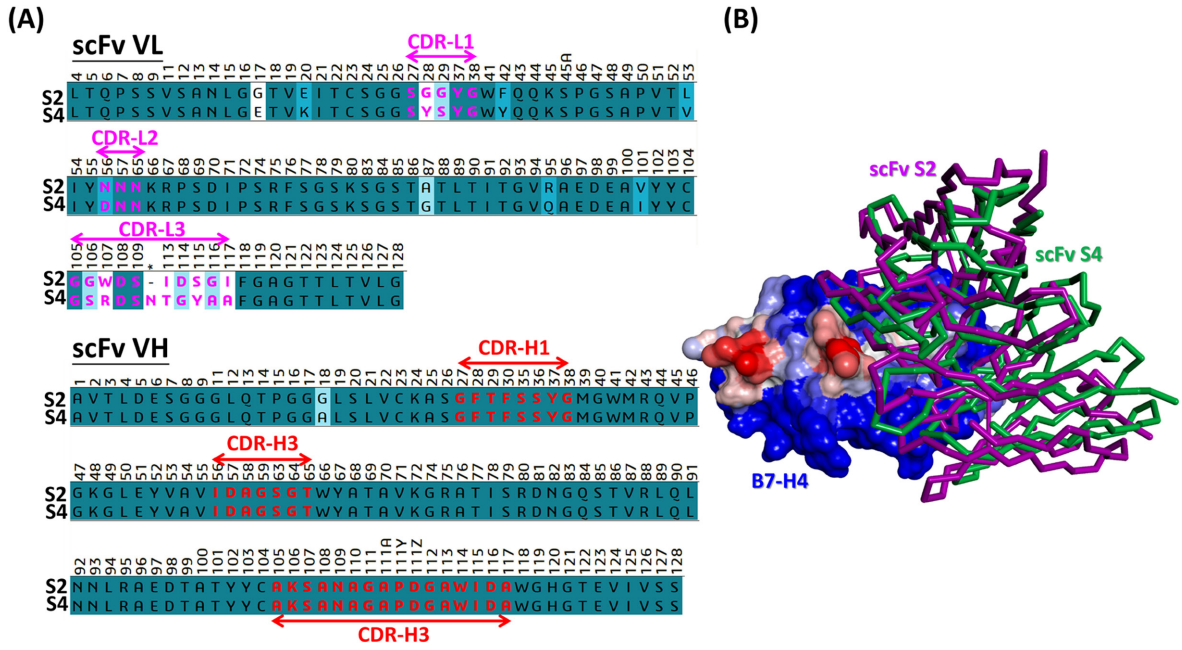

Fig. 5. Sequence analysis of scFv S2 and scFv S4 and their molecule docking with B7-H4. (A) Sequence analysis and comparison of scFv S2 and scFv S4 including VL and VH regions. The background of the residues is colored according to sequence similarity. The deep color shows the conserved residues in all sequences. The color scheme is from deep to light, corresponding to identity, highly conserved residues, and low-conserved residues, respectively. The residue backgrounds colored in white are not similar. Residues of the CDRs are indicated by bold letters with arrow marks (purple in VL and red in VH). (B) Molecule docking of scFv S2 and scFv S4 with B7-H4 according to the confirmed epitope position on B7-H4 for overlay analysis.

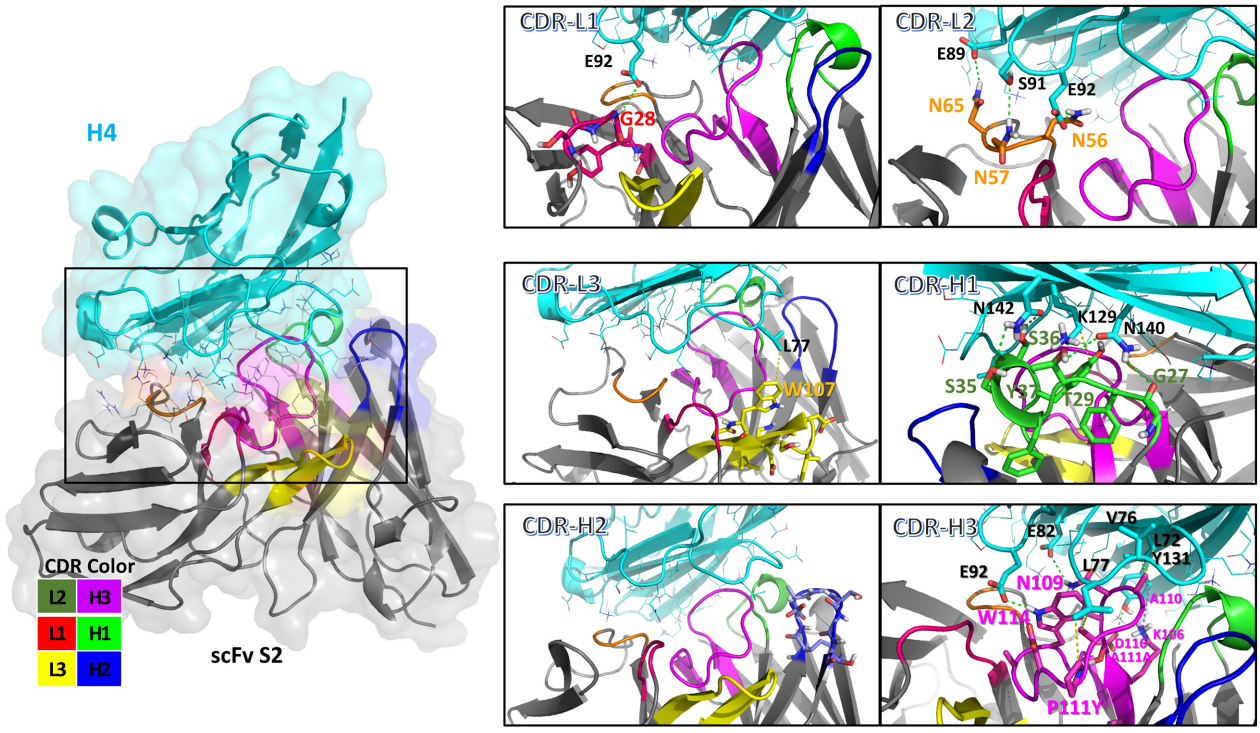

Fig. 6. Molecular modeling of scFv S2 and B7-H4 interaction and secondary structure for scFv S2 antibody–B7-H4 antigen model. The B7-H4 antigen and scFv S2 are colored light cyan and gray, respectively. Schematic of all interactions between scFv S2 and the B7-H4 epitope. The interface residues of scFv S2 and B7-H4 were concentrated on the CDR-L1 (red), CDR-L2 (orange), CDR-L3 (yellow), CDR-H1 (green), CDR-H2 (blue), and CDR-H3 (magenta) loops. The interaction between scFv S2 and B7-H4 is illustrated using green, yellow, and magenta dotted lines to indicate hydrogen bonds, hydrophobic interactions, and cation-pi interactions, respectively.

with the B7-H4 epitope. The side chain of Ala110 on the CDR-H3 loop interacted with those of Val76 and Leu72 through hydrophobic interactions. The side chains of Lys106 and Asp116 on the CDR-H3 loop interacted with that of Tyr131 through cation-pi interaction and a hydrogen bond. Moreover, the Ala110A and Pro111Y side chains on the CDR-H3 loop interacted with the side chain of Leu77 through hydrophobic interactions. The side chains of Trp114 and Asn109 also interacted with those of Glu92 and Glu82 through two hydrogen bonds.

Discussion

Although clinical therapeutic strategies using immune checkpoints have already been proven effective, most patients may have primary resistance and fail to benefit from the treatment. Additionally, users of certain medication may experience tumor recurrence after the initial response; this may be a response caused by the body generating systemic acquired resistance [26, 27]. Therefore, various uncertainties remain in regulating immunotherapy, and they require resolutions. Because it is highly complicated, the tumor microenvironment causes the regulation of immune checkpoints to vary. Even in the same patient, treatment of metastatic meningioma in various body parts may yield heterogeneous treatment effects. Tumor microenvironments consist of various factors that are conducive to resistance development; for example, the expression of other inhibitory immune checkpoint molecules enables tumors to escape immune responses [27, 28]. Therefore, the development of new immune checkpoint indicators for immunotherapy is urgent. Studies have reported that expression of B7-H4 protein in cancer tissues is highly correlated with cancer stage, patient survival rate, and the invasiveness of T-cells in the tumor [14]. Notably, the number of B7-H4 molecules on the surface of cancer strains significantly drops after long durations of artificial culturing. Changes in the cultivation conditions to enhance the severity of the growth environment can induce the expression of B7-H4 protein [29]. Additionally, researchers discovered that the surfaces of cancer cells in the ascites and on solid tumors of patients with cancer exhibited high B7-H4 expression. However, after short sessions of *in vitro* cultivation, B7-H4 expression on the cell surface significantly dropped [30]. These findings suggest that the expression of B7-H4 protein on cell surfaces is influenced and regulated by the environment and may be related to *in vivo* tumor cells enhancing their resistance to avoid immune recognition [31].

Individual differences among species have resulted in uncertainties concerning the treatment responses of immune checkpoints. Therefore, being able to predict immune response prior to treatment is key. However, uncertainties in the efficacy of using specific biomarkers to predict treatment effects and treatment-induced toxic reactions remain unresolved. Despite the fact that multiple novel immune checkpoint molecules have been determined to be potential indicators, most agents do not have specific accompanying biomarkers for validation. Currently, the two biomarkers employed for predicting immune reactions, namely PD-L1 and mismatch repair (MMR), have already been approved by the U.S. FDA and can be applied alongside checkpoint inhibitor agents. However, PD-L1 expression and MMR deficiency cannot encompass all reactions to predict the response of patients with physical tumors to immune checkpoint inhibitor agents and cannot be used to predict the medication effect on a patient or the response duration. Studies have indicated that in addition to the abnormal expression of B7-H4 on cancer cell surfaces, soluble B7-H4 (sB7-H4) molecules are present in the serum of patients with cancer [11, 12]. Additionally, the presence of sB7-H4 was correlated with tumor size, lymphatic metastasis, and tumor invasion depth [11]. Indeed, we discovered an increase in sB7-H4 in the culture medium of cancer cells that expressed B7-H4 (data not shown). These findings are highly conducive to the development of B7-H4-specific inhibitor agents, which may be applied in clinical practice alongside diagnosis to achieve optimal treatment results.

In the present study, the isolated anti-B7-H4 antibody successfully inhibited the B7-H4 protein-induced immunosuppression effect and enabled the successful activation of T-cells in PBMCs through effective stimulation. Therefore, we conclude the isolated antibody bound to effective epitopes on B7-H4 proteins to block the binding between B7-H4 and receptor proteins. Through molecule docking analysis, we discovered that scFv S4 mainly relies on the VH domain to bind to B7-H4 protein. This finding is similar to the effect of the anti-PDL1 clinical antibody drug Atezolizumab in complex structures [32]. This implies that in the antibody response of some immune checkpoint inhibitor agents, the VH domain could be the main binding site and VL domain plays the role of stabilizing the antibody structure. In our experiment, we discovered that immunized mice cannot be induced to generate effective humoral antibody responses because B7-H4 proteins in mammals have high sequence similarity (Fig. 1). Therefore, for our immune animal hosts, we used chickens instead of mice. Due to difference in species, mammalian proteins can generate higher immunity responses in chicken and are more likely to stimulate more instances of somatic mutation.

After genetic sequence analysis, in which the germline sequences in chicken were compared, we discovered that the somatic mutations that occurred in the sequence of isolated antibodies S2 and S4 were mainly caused by the insertion mutation (Supplementary Fig. 1). This finding is similar to that of our previous research [23]. This occurrence of mutation with high variability generates longer CDR3-H3 loops, which are capable of entering deeper regions of the antigen epitope.

The use of immunotherapy to treat cancer has achieved some positive results, but remains for improvement. The anti-B7-H4 antibody which is specific to immunity checkpoint protein has the potential to be applied with existing treatment strategies to enhance the treatment effect. Therefore, this antibody can be used as an auxiliary measure to overcome the problem of immune cell failure during tumor immune escape and thus provides more treatment options for the future development of anticancer medicine.

Conflicts of Interest

none

Acknowledgment

This work was financially supported by the "TMU Research Center of Cancer Translational Medicine" from The Featured Areas Research Center Program within the framework of the Higher Education Sprout Project by the Ministry of Education (MOE) in Taiwan and the Ministry of Science and Technology in Taiwan under Grant MOST 108-2320-B-038-065. We also thank the Department of Psychiatry at Kaohsiung Armed Forces General Hospital for its participation in this study under Grant KAFGH_D_109034.

Reference

1. Chen DS, Mellman I. Elements of cancer immunity and the cancer-immune set point. Nature. 2017; 541: 321–330. [Medline] [CrossRef]
2. Page DB, Postow MA, Callahan MK, Allison JP, Wolchok JD. Immune modulation in cancer with antibodies. Annu Rev Med. 2014; 65: 185–202. [Medline] [CrossRef]
3. Zang X, Loke P, Kim J, Murphy K, Waitz R, Allison JP. B7x: a widely expressed B7 family member that inhibits T cell activation. Proc Natl Acad Sci USA. 2003; 100: 10388–10392. [Medline] [CrossRef]
4. Sica GL, Choi IH, Zhu G, Tamada K, Wang SD, Tamura H, et al. B7-H4, a molecule of the B7 family, negatively regulates T cell immunity. Immunity. 2003; 18: 849–861. [Medline] [CrossRef]
5. Chen C, Qu QX, Shen Y, Mu CY, Zhu YB, Zhang XG, et al. Induced expression of B7-H4 on the surface of lung cancer cell by the tumor-associated macrophages: a potential mechanism of immune escape. Cancer Lett. 2012; 317: 99–105. [Medline] [CrossRef]
6. Prasad DV, Richards S, Mai XM, Dong C. B7S1, a novel B7 family member that negatively regulates T cell activation. Immunity. 2003; 18: 863–873. [Medline] [CrossRef]
7. Dong Q, Ma X. B7-H4 expression is associated with tumor progression and prognosis in patients with osteosarcoma. BioMed Res Int. 2015; 2015: 156432. [Medline] [CrossRef]
8. Maskey N, Li K, Hu M, Xu Z, Peng C, Yu F, et al. Impact of neoadjuvant chemotherapy on lymphocytes and co-inhibitory B7-H4 molecule in gastric cancer: low B7-H4 expression associates with favorable prognosis. Tumour Biol. 2014; 35: 11837–11843. [Medline] [CrossRef]
9. Peng HX, Wu WQ, Yang DM, Jing R, Li J, Zhou FL, et al. Role of B7-H4 siRNA in Proliferation, Migration, and Invasion of LOVO Colorectal Carcinoma Cell Line. BioMed Res Int. 2015; 2015: 326981. [Medline] [CrossRef]
10. Zhu J, Chu BF, Yang YP, Zhang SL, Zhuang M, Lu WJ, et al. B7-H4 expression is associated with cancer progression and predicts patient survival in human thyroid cancer. Asian Pac J Cancer Prev. 2013; 14: 3011–3015. [Medline] [CrossRef]
11. Shi H, Ji M, Wu J, Zhou Q, Li X, Li Z, et al. Serum B7-H4 expression is a significant prognostic indicator for patients with gastric cancer. World J Surg Oncol. 2014; 12: 188. [Medline] [CrossRef]
12. Xu C, Qian L, Yu L, Zhang X, Wang Q. Evaluation of serum and pleural levels of soluble B7-H4 in lung cancer patients with pleural effusion. Biomarkers. 2015; 20: 271–274. [Medline] [CrossRef]
13. Krambeck AE, Thompson RH, Dong H, Lohse CM, Park ES, Kuntz SM, et al. B7-H4 expression in renal cell carcinoma and tumor vasculature: associations with cancer progression and survival. Proc Natl Acad Sci USA. 2006; 103: 10391–10396. [Medline] [CrossRef]
14. Kryczek I, Wei S, Zhu G, Myers L, Mottram P, Cheng P, et al. Relationship between B7-H4, regulatory T cells, and patient outcome in human ovarian carcinoma. Cancer Res. 2007; 67: 8900–8905. [Medline] [CrossRef]
15. Xu Y, Zhu S, Song M, Liu W, Liu C, Li Y, et al. B7-H4 expression and its role in interleukin-2/interferon treatment of clear cell renal cell carcinoma. Oncol Lett. 2014; 7: 1474–1478. [Medline] [CrossRef]
16. Groves DJ, Morris BA. Veterinary sources of nonrodent monoclonal antibodies: interspecific and intraspecific hybridomas. Hybridoma. 2000; 19: 201–214. [Medline] [CrossRef]
17. Barbas CF 3rd, Kang AS, Lerner RA, Benkovic SJ. Assembly of combinatorial antibody libraries on phage surfaces: the gene III site. Proc Natl Acad Sci USA. 1991; 88: 7978–7982. [Medline] [CrossRef]
18. Rahbarnia L, Farajnia S, Babaei H, Majidi J, Veisi K, Ahmadzadeh V, et al. Evolution of phage display technology: from discovery to application. J Drug Target. 2017; 25: 216–224. [Medline] [CrossRef]
19. Shim H. Therapeutic Antibodies by Phage Display. Curr Pharm Des. 2016; 22: 6538–6559. [Medline] [CrossRef]
20. Andris-Widhopf J, Rader C, Steinberger P, Fuller R, Barbas CF 3rd. Methods for the generation of chicken monoclonal antibody fragments by phage display. J Immunol Methods. 2000; 242: 159–181. [Medline] [CrossRef]
21. Finlay WJ, Shaw I, Reilly JP, Kane M. Generation of high-affinity chicken single-chain Fv antibody fragments for measurement of the Pseudonitzschia pungens toxin domoic acid. Appl Environ Microbiol. 2006; 72: 3343–3349. [Medline] [CrossRef]
22. Li C, He J, Ren H, Zhang X, Du E, Li X. Preparation of a Chicken scFv to Analyze Gentamicin Residue in Animal Derived Food Products. Anal Chem. 2016; 88: 4092–4098. [Medline] [CrossRef]
23. Tsai KC, Chiang CW, Lo YN, Chang FL, Lin TY, Chang CY, et al. Generation and characterization of avian-derived anti-

human CD19 single chain fragment antibodies. Anim Biotechnol. 2019; 30: 293–301. [Medline] [CrossRef]
24. Nishibori N, Horiuchi H, Furusawa S, Matsuda H. Humanization of chicken monoclonal antibody using phage-display system. Mol Immunol. 2006; 43: 634–642. [Medline] [CrossRef]
25. Akita EM, Nakai S. Production and purification of Fab' fragments from chicken egg yolk immunoglobulin Y (IgY). J Immunol Methods. 1993; 162: 155–164. [Medline] [CrossRef]
26. Kelderman S, Schumacher TN, Haanen JB. Acquired and intrinsic resistance in cancer immunotherapy. Mol Oncol. 2014; 8: 1132–1139. [Medline] [CrossRef]
27. Sharma P, Hu-Lieskovan S, Wargo JA, Ribas A. Primary, Adaptive, and Acquired Resistance to Cancer Immunotherapy. Cell. 2017; 168: 707–723. [Medline] [CrossRef]
28. Jenkins RW, Barbie DA, Flaherty KT. Mechanisms of resistance to immune checkpoint inhibitors. Br J Cancer. 2018; 118: 9–16. [Medline] [CrossRef]
29. Iizuka A, Kondou R, Nonomura C, Ashizawa T, Ohshima K, Kusuhara M, et al. Unstable B7-H4 cell surface expression and T-cell redirection as a means of cancer therapy. Oncol Rep. 2016; 36: 2625–2632. [Medline] [CrossRef]
30. Dangaj D, Lanitis E, Zhao A, Joshi S, Cheng Y, Sandaltzopoulos R, et al. Novel recombinant human b7-h4 antibodies overcome tumoral immune escape to potentiate T-cell antitumor responses. Cancer Res. 2013; 73: 4820–4829. [Medline] [CrossRef]
31. Pardoll DM. The blockade of immune checkpoints in cancer immunotherapy. Nat Rev Cancer. 2012; 12: 252–264. [Medline] [CrossRef]
32. Lee HT, Lee JY, Lim H, Lee SH, Moon YJ, Pyo HJ, et al. Molecular mechanism of PD-1/PD-L1 blockade via anti-PD-L1 antibodies atezolizumab and durvalumab. Sci Rep. 2017; 7: 5532. [Medline] [CrossRef]